Hindawi
Geofluids
Volume 2023, Article ID 6333122, 13 pages
https://doi.org/10.1155/2023/6333122

Research Article

Investigation of the Impact of Leaching Agent Concentration and pH on the Stability of Agglomeration of Ion-Absorbed Rare Earth Deposits

Zhongquan Gao,[1] Yunzhang Rao,[1] Liang Shi,[2] Xiaoming Zhang,[2] and Run Xiang[1]

[1]*School of Resources and Environmental Engineering, Jiangxi University of Science and Technology, Ganzhou 341000, China*
[2]*School of Architectural and Surveying & Mapping Engineering, Jiangxi University of Science and Technology, Ganzhou 341000, China*

Correspondence should be addressed to Yunzhang Rao; raoyunzhang@jxust.edu.cn

Received 16 February 2023; Revised 1 September 2023; Accepted 19 September 2023; Published 25 October 2023

Academic Editor: Dan Ma

Ion-absorbed rare earth deposits react with the leaching agent during the *in situ* leaching process through ion exchange and hydration, which change the stability of ore agglomerates and even result in mining slopes or landslides. Indoor simulated column leaching assays were conducted on ion-absorbed rare earth deposit samples by using magnesium sulfate solution as the leaching solution. Surface zeta potential, double electric layer thickness, particle gradation, and pore structure were analyzed to measure the different concentrations and pHs of leaching solutions' impact on the stability of ore agglomerates. Results show that the critical magnesium sulfate solution concentration and pH affecting the stability of deposit sample agglomerates are 3.5% and 4, respectively. The chemical replacement reaction between the leaching agent and rare earth ions occurs during column leaching when it reaches its zero-point potential at a pH of 3.5168. This breaks the balance between the van der Waals gravitational force and double-layer repulsion in clay particles and induces the disruption of agglomerates, which causes the difference in the pore radius ratio of the ore samples before and after column leaching. It is of great engineering guidance to solve the problems of slope instability and landslides that may occur in the ore body during the mining process of ionic rare earth ore.

1. Introduction

Ion-absorbed rare earth deposits are an important resource in the world and widely used in aerospace, machinery, electronics, medical, health care, and transportation [1], which have a significant impact on the development of new materials and the new energy industry. Southern China's ion-absorbed rare earth deposits are found as hydrated cations or hydroxyl hydrated cations [2], which are distinguished by their complete composition, abundance, and high content of medium and heavy rare earth [3]. The mechanism of the *in situ* leaching process is that the rare earth deposit cations adsorbed on the clay surface are desorbed by more active cations (H^+, NH^{4+}) into the solution [4]. Compared to pool leaching and heap leaching, *in situ* leaching has the highest resource recovery rate, the lowest cost [5], and the least workload. However, mining for rare earth resources also entails unavoidable environmental issues [6]; ammonia nitrogen residues contaminate water sources seriously [7, 8], protracted leaching reduces the soil's shear strength and increases its pore structure [9], which causes slope instability [10], landslides, and rare earth tailing. The basic building blocks of soil structure are called agglomerates; several researchers have provided a quantitative overview of three agglomerate dynamic processes: agglomeration, stabilization, and dispersion [11–14]. Agglomerate stability affects the fragmentation and particle size distribution of the broken agglomerates during the erosion process. Salt solutions may also affect soil physicochemical properties by changing the interaction between soil minerals and organic matter,

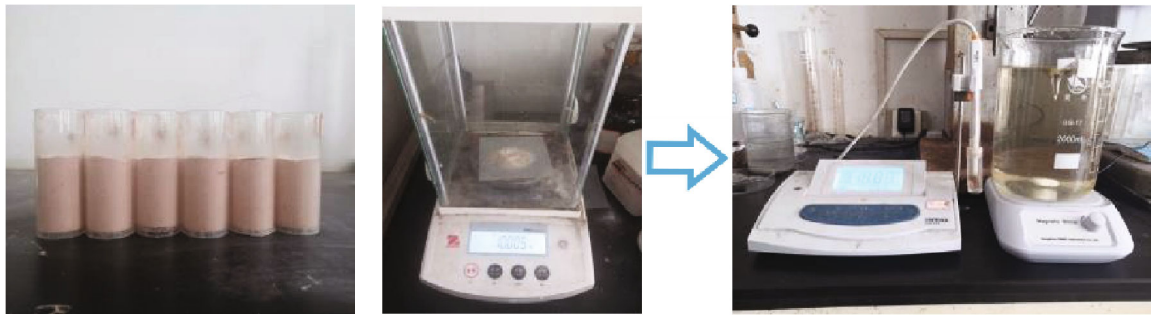

(a) (b)

Figure 1: Experimental materials and instruments. (a) Rare earth samples. (b) Reagents.

thus reducing the affinity between agglomerate particles, changing the soil agglomerates' particle size composition [15, 16], and inducing agglomerates' structural changes. Ma et al. showed that seepage has an important effect on particle transport, resulting in large changes in hydraulic properties [17–19]. Caron et al. showed that changes in the ionic strength alter the interaction forces (electrostatic repulsion, hydration repulsion, and van der Waals gravity) between soil particles and play a key role in the soil particles' agglomeration and dispersion that affect its structural stability [20]. Curtin et al. suggested that the mucilage particles show different degrees of dispersion or flocculation depending on the properties of Ca^{2+} or Mg^{2+} [21], and the agglomerate stability was negatively correlated with the montmorillonite/kaolinite ratio and positively correlated with the Ca^{2+}/Mg^{2+} ratio and iron aluminum oxide [22]. The cementation effect generated by Ca^{2+} inhibits the dissolution of calcareous cement and clay mineral production in the soil [23], raising the charge on the soil surface and the ion exchange between Na^{+}, K^{+}, and solution Ca^{2+} [24], thus increasing the interparticle affinities and the tight conjunction of particles that induce smaller soil pores, tighter particles, and stabler soil structures. Wang et al. showed that during the leaching process, complex chemical reactions occur, causing changes in the pore structure within the ore body [25–27]. Hu et al. found that the electrostatic repulsive force is affected by various factors, including the type of electrolyte, concentration, pH, and others [28, 29]. This results in a change in the sliding layer thickness on the soil particles' surface diffusion double layer, which alters the thickness of the adsorbed water film and causes harm to the leaching agents' infiltration direction and particle migration [30].

To address the issues of slope instability and landslides that may arise in the ion-absorbed rare earth deposits during the mining process, it is crucial to consider the effects of different leaching agent concentrations and pHs on the stability of ion-absorbed rare earth deposits agglomerates. In this study, by using different concentrations and pHs of magnesium sulfate leaching solutions, we noticed that the changes in the surface potential and sliding layer thickness in the diffusion double layer of mineral particles can affect the agglomerates' structural stability by altering mineral particles' interaction forces in the ion exchange reaction, in which Mg^{2+} desorbs RE^{3+} in the ion-absorbed rare earth deposits sample.

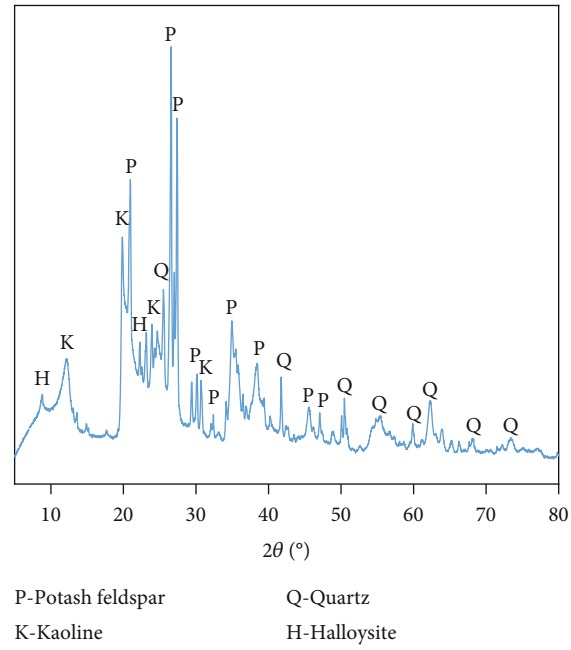

Figure 2: XRD spectra of the rare earth sample.

2. Materials and Methods

2.1. Materials. Figure 1(a) depicts the rare earth specimens used in the assay, which were obtained from the rare earth mine in Longnan County, Ganzhou City. Figure 2 displays the rare earth sample X-ray diffraction (XRD) spectra. The collected *in situ* soils were tested in the laboratory for particle gradation, as shown in Table 1. Seven sets of magnesium sulfate solutions with different mass percent concentrations of 2.0%, 2.5%, 3.0%, 3.5%, 4.0%, 4.5%, and 5.0%, and five sets of magnesium sulfate solutions with 3.5% concentrations of pH 2, 3, 4, 5, and 6, respectively, were prepared for indoor simulated column leaching tests. By using the electronic balance to measure the precise mass of magnesium sulfate in deionized water and adjusting the volume to 1 L to generate the corresponding mass percent concentrations of magnesium sulfate solution, different pHs magnesium sulfate solutions were obtained by adding 2% dilute sulfuric acid to adjust the acidity of the solution to a concentration of 3.5% by pH meter.

Table 1: Particle gradation of the *in situ* rare earth soils.

Particle diameter (mm)	>5	2.5-5	1-2.5	0.5-1	0.075-0.5	<0.075
Percentage (%)	12.8	28.9	7.3	8.4	28.7	13.9

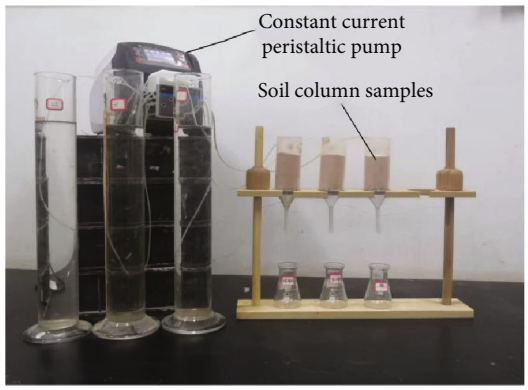

Figure 3: Indoor simulation of column leaching.

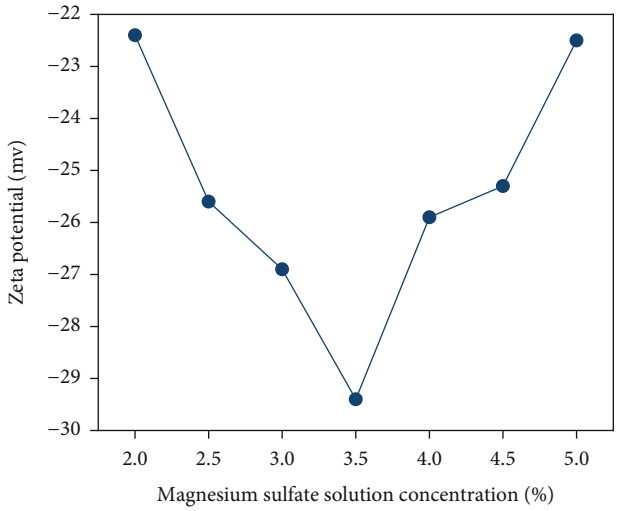

Figure 4: The concentration of leaching solution influences the surface zeta potential of rare earth particles.

2.2. Methods. The indoor simulated column leaching method for ion-absorbed rare earth deposits was used and strictly implemented, referring to the standard of remodeled soil samples. The column apparatus was made of an acrylic tube of 44 mm inner diameter and 2 mm wall thickness, as shown in Figure 3. According to the effective range of nuclear magnetic resonance detection, the diameter-to-height ratio of the remodeled soil sample was 44 : 60. The stability and structural change of ion-absorbed rare earth deposits agglomerates were measured under different concentrations and pHs of magnesium sulfate solution treatment after leaching.

Soil sample remodeling of rare earth samples is a dynamic desorption process with a large number of ion exchange reactions occurring within the column leaching process. This is done by loading the column with the pre-weighed rare earth samples while using the peristaltic pump

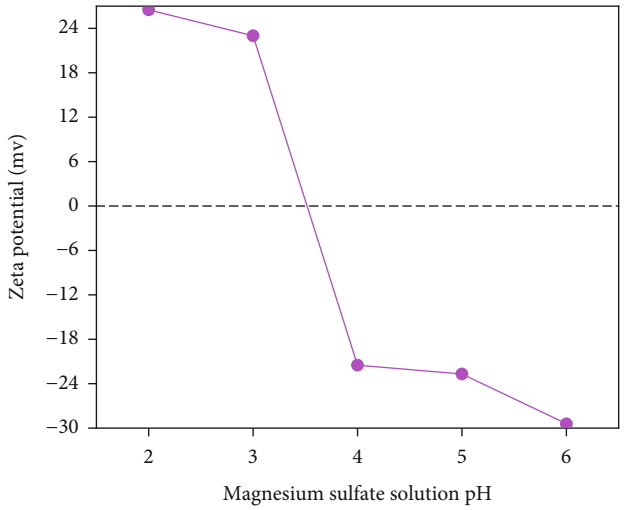

Figure 5: The pH of the leaching solution influences the surface zeta potential of rare earth particles.

to adjust the liquid injection flow rate, then collecting the leaching solution for testing after each leaching and obtaining the required data. During leaching, the ion exchange happened between Mg^{2+} in the solution and RE^{3+} in the ore sample, which changed the thickness of the sliding layer on the surface of the ore particles. According to the theory of the diffusion double layer model, zeta potential is used to characterize the stability of colloids [31], which reflects the adsorption state of colloids with ions. Therefore, the zeta potential of colloidal particles was determined by using the zetaprobe potential analyzer from Colloidal Dynamics, USA. The pore structure parameters of the leached specimens can be quickly and nondestructively determined by the NM-60 magnetic resonance rock microstructure instrument (Suzhou Niumag Analytical Instrument Corporation, MESOMR23 model) and further obtained from the T_2 distribution curve of each leached specimen. By testing the porosity and different pore sizes of the specimens during column leaching, the evolution of the internal pore structure can be dynamically analyzed from a microscopic perspective. The rare earth ore sample and the leaching solution undergo water-earth chemical interaction during column leaching; thus, the particles in the rare earth ore sample are agglomerated or dispersed with a certain water content after leaching, and their size distribution was measured by the Winner 2000 laser particle size analyzer.

3. Results and Discussion

3.1. The Surface Zeta Potential of Rare Earth Particles Influenced by the Concentration and pH of the Leaching Solution. Magnesium sulfate solutions with seven different

Table 2: Basic parameters of ore samples.

Designation		Zeta potential	D50 (μm)	Particle specific surface area (m^2/g)
Magnesium sulfate solution Concentration (%)	2.0	-22.4	35.592	0.351
	2.5	-25.6	33.828	0.363
	3.0	-26.9	34.127	0.374
	3.5	-29.4	32.195	0.372
	4.0	-25.9	33.925	0.379
	4.5	-25.3	33.882	0.378
	5.0	-22.5	35.881	0.356
Magnesium sulfate solution pH	2	26.5	35.998	0.348
	3	23.0	38.456	0.321
	4	-21.5	36.925	0.323
	5	-22.7	34.483	0.351
	6	-29.4	32.195	0.372

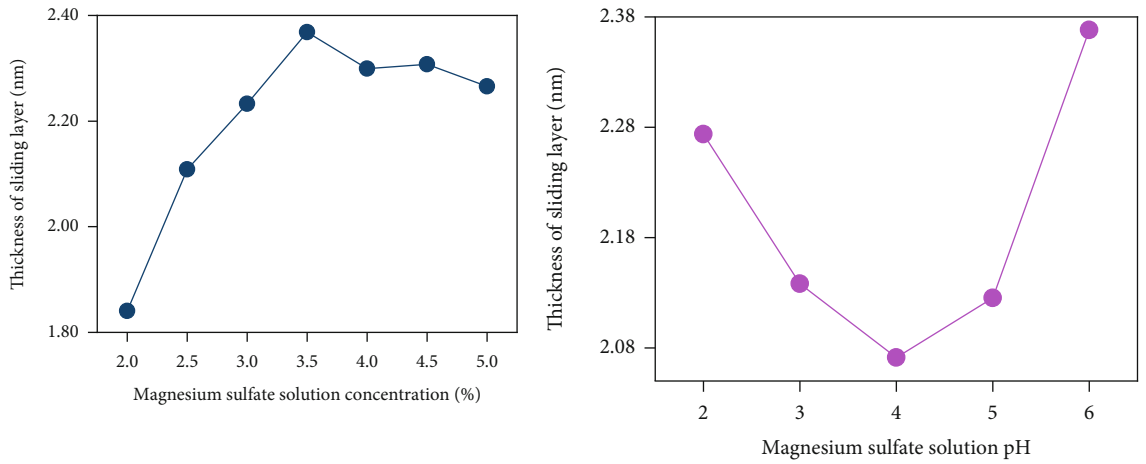

Figure 6: The concentration and pH of the leaching solution influence the surface sliding layer thickness of rare earth particles. (a) Different leaching solution concentrations. (b) Different leaching solution pHs.

mass percent concentrations of 2.0%, 2.5%, 3.0%, 3.5%, 4.0%, 4.5%, and 5.0% were prepared for the indoor simulated column leaching test, respectively. By measuring the zeta potential on the surface of rare earth particles, the effect of different concentrations of the leaching solution was systematically analyzed. The leaching process of ionic rare earth ores is not spontaneous but relies on the concentration difference between two ions exchanging. As shown in Figure 4, with a lower cation concentration range in the leaching solution, the absolute value of the zeta potential is gradually increasing along with the increased cation concentration in the solution. The zeta potential is -29.4 mv when the Mg^{2+} concentration reached 3.5%, compared with the absolute value of the zeta potential increasing by 31.25% with 2.0% of the Mg^{2+} concentration. This is because of the preferential chemical reaction of Mg^{2+} with RE^{3+} in rare earth ore; that is, a large amount of Mg^{2+} will adsorb to the inner layer of the diffusion double layer due to the electrostatic effect, which induces a change in zeta potential. With more cations entering into the diffusion double layer, the stronger the potential energy is, which makes the absolute value of zeta potential further increases. However, the absolute value of zeta potential decreases with the increase in leaching cation concentration when Mg^{2+} concentration exceeds 3.5%. As the cation concentration increases and the cation ions enter the diffusion double layer, the counter ions with the same charge in the diffusion layer were pressed into the adsorption layer, which results in the compressed diffusion layer. While the replacement reaction with RE^{3+} occurs, a chemical reaction with impurity ions such as Ca^{2+} in rare earth ore also happens, causing a slower replacement rate of RE^{3+} ions than the rate of particle surface adsorbed impurity ions, which induces a gradual decrease in the absolute value of zeta potential on the particle surface.

Prepare 3.5% magnesium sulfate solutions with different pHs (2, 3, 4, 5, and 6) for column leaching assays. As shown in Figure 5, solution pH has a large influence on the zeta potential. The surface zeta potential of rare earth ore particles decreases with the increased solution pH and undergoes a trend from positive to negative, followed by a gradually

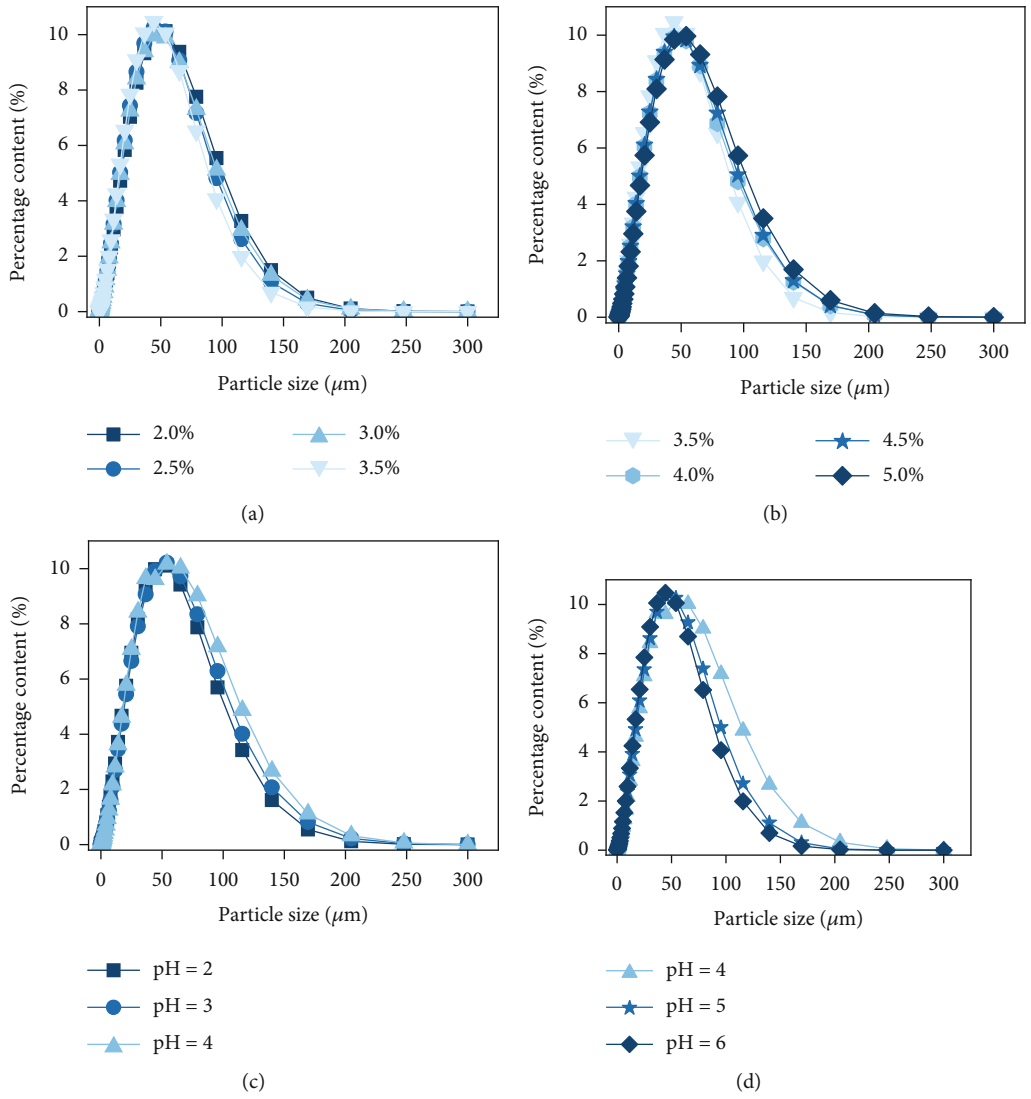

Figure 7: The concentration and pH of the leaching solutions influence the particle size distribution of ore samples. (a) Leaching solution concentrations range from 2.0% to 3.5%. (b) Leaching solution concentrations range from 3.5% to 5.0%. (c) Leaching solution pH range from 2 to 4. (d) Leaching solution pH range from 4 to 6.

increased absolute value. When pH increased from 2 to 6, the zeta potential changed from 26.5 mv to -29.4 mv, with a change of 55.9 mv, and reached its zero point potential at the pH of 3.5168. The charge on the Stern layer is firmly bound to the colloidal particles, while the charge on the sliding layer varies with the pH. When pH decreases, the negative charge on the sliding layer reacts with the added H^+, which increases the potential of the sliding layer, so that the zeta potential increases with the decreased pH consequently [31]. During leaching, Mg^{2+} is switched with the rare earth ions by ion exchange. When pH < 3.5168, the attraction force between the clay colloidal particles and Mg^{2+} turns into repulsion because of the positive zeta potential, and H^+ is adsorbed by the surface of rare earth ore, resulting in a gradually increased zeta potential. When 3.516 < pH < 6, the surface charge of rare earth particles and zeta potential is negative due to the generation of a large number of -OH groups by rare earth ore in a weakly acidic environment, while the counter ions of the Stern layer in the solution are positive. With the reduced pH, solution H^+ increases and reacts with the -OH group by neutralizing the surface of the particles. Because of the added H^+, the negative charge on the sliding layer of rare earth colloids decreased and attenuated its attraction to Mg^{2+}, which deduced its ability to enter the sliding layer and exchange with rare earth ions, which eventually caused the compressed diffusion double electric layer with the decreased absolute value of the zeta potential on the particle surface.

3.2. The Stability of Rare Earth Ore Agglomerates Influenced by the Concentration and pH of the Leaching Solution. When changing the concentration and pH of the leaching solution, the particle surface potential, zeta potential, and the type of ions were significantly changed, resulting in a shift in the sliding layer thickness of the double electric layer on the particle surface [32]. To calculate the thickness of the sliding

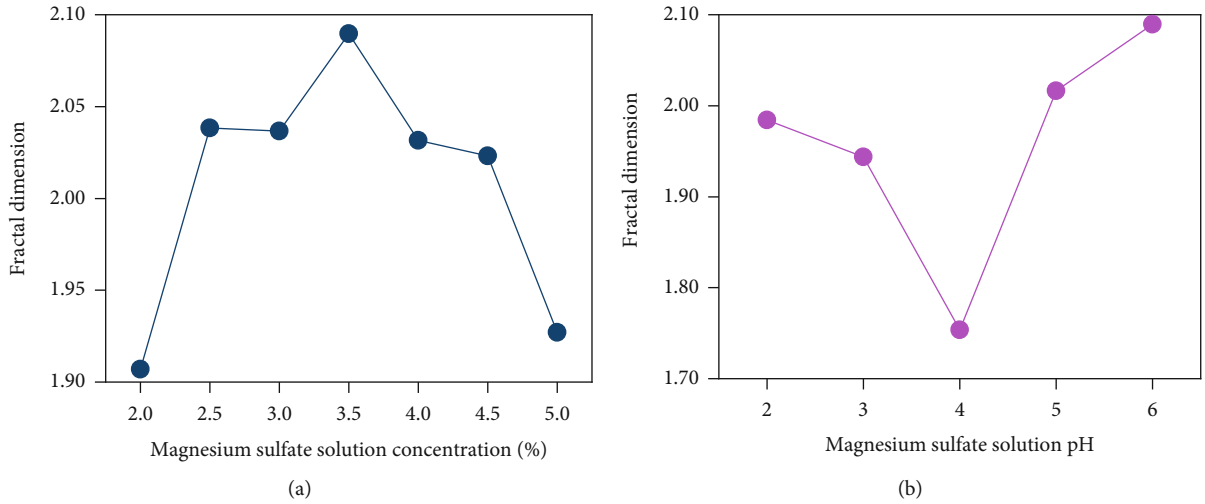

Figure 8: The concentration and pH of the leaching solution influence the fractal dimension distribution curve of ore samples. (a) Different leaching solution concentrations. (b) Different leaching solution pHs.

layer, the zeta potential and specific surface area of each ore particle sample were determined after leaching with different concentrations and pHs of magnesium sulfate solution, as shown in Table 2. It is known that $MgSO_4$ is a 2 : 2 type electrolyte solution [33], and the Gouy-Chapman equation describes the relationship between the sliding surface potential and distances in a single electrolyte system. Therefore, for the 2 : 2 type single electrolyte solution system, the calculated equation for the sliding layer thickness in the double layer on the surface of the ore particles is shown as follows:

$$x_s = \frac{1}{k} \ln \left[\frac{8 + 8e^{\zeta F/\mathrm{RT}}}{\lambda\left(1 - e^{\zeta F/\mathrm{RT}}\right)} \right]. \tag{1}$$

In the equation, F stands for Faraday's constant ($F = 96490$ C/mol); R is the gas constant ($R = 8.314$ J/mol·K); T is the absolute temperature (K); ζ is the zeta potential, unit in V; λ denotes as a constant; and k denotes as the Debye shock constant. The expressions of λ and k are shown as follows:

$$\lambda = \frac{8 + 8e^{F\psi_0/\mathrm{RT}}}{\lambda\left(1 - e^{F\psi_0/\mathrm{RT}}\right)}, \tag{2}$$

$$k = \sqrt{\frac{32\pi F^2 Z^2 c_c}{\varepsilon \mathrm{RT}}}. \tag{3}$$

In the equation, ψ_0 denotes the charged particle Stern potential calculated from the reference [34], unit in V; ε stands for the dielectric constant of the medium; Z is the valence of the cation in the 2 : 2 electrolyte system; and c_c is the concentration of the cation in the 2 : 2 electrolyte system, unit in mol/L.

As shown in Figure 6(a), when the concentration of magnesium sulfate solution increased from 2.0% to 3.5%, the thickness of the sliding layer on the surface of the ore sample particles increased from 1.840 nm to 2.368 nm; when the concentration increased from 3.5% to 5.0%, the sliding layer thickness decreased from 2.368 nm to 2.266 nm. Figure 6(b) shows that the sliding layer thickness dropped from 2.274 nm to 2.071 nm when the pH of the magnesium sulfate solution increased from 2 to 4. However, the thickness enhanced from 2.071 nm to 2.368 nm when the pH increased from 4 to 6.

The application of fractal theory began in the early 1980s. Soil is a system of porous media with similar structure and fractal characteristics, also involving soil aggregates, chemical reaction interfaces, and the fractal dimension of soil pores. The fractal dimension of ore particles is a parameter that describes the size of ore body particles as a whole based on the size distribution of ore particles. The fractal model of ion-absorbed rare earth deposits agglomerate structure based on fractal theory is shown in the following [5]:

$$D_f = -\lim \frac{\ln N(r)}{\ln r}. \tag{4}$$

In the equation, N stands for the total number of ore clay, while r denotes the particle size. In the double logarithmic curve of $\ln N(r) - \ln r$, D_f is the fractal dimension of the ore agglomerate distribution.

Agglomerates with particle sizes between 53 μm and 250 μm are micro agglomerates, and those less than 53 μm are viscous agglomerates [35]. The rare earth ore samples below 0.075 mm after column leaching were vibrated and sieved out. The particle size distribution curves of the ore samples being leached with different concentrations and pHs of magnesium sulfate solution are shown in Figure 7. The fractal dimension of each particle after leaching was calculated according to Equation (4) and shown in Figure 8.

As shown in Figures 7(a), 7(b), and 8(a), when the concentration of magnesium sulfate solution increases from 2.0% to 3.5%, the percentage of viscous agglomerates (below 53 μm) increases while micro agglomerates (above 53 μm)

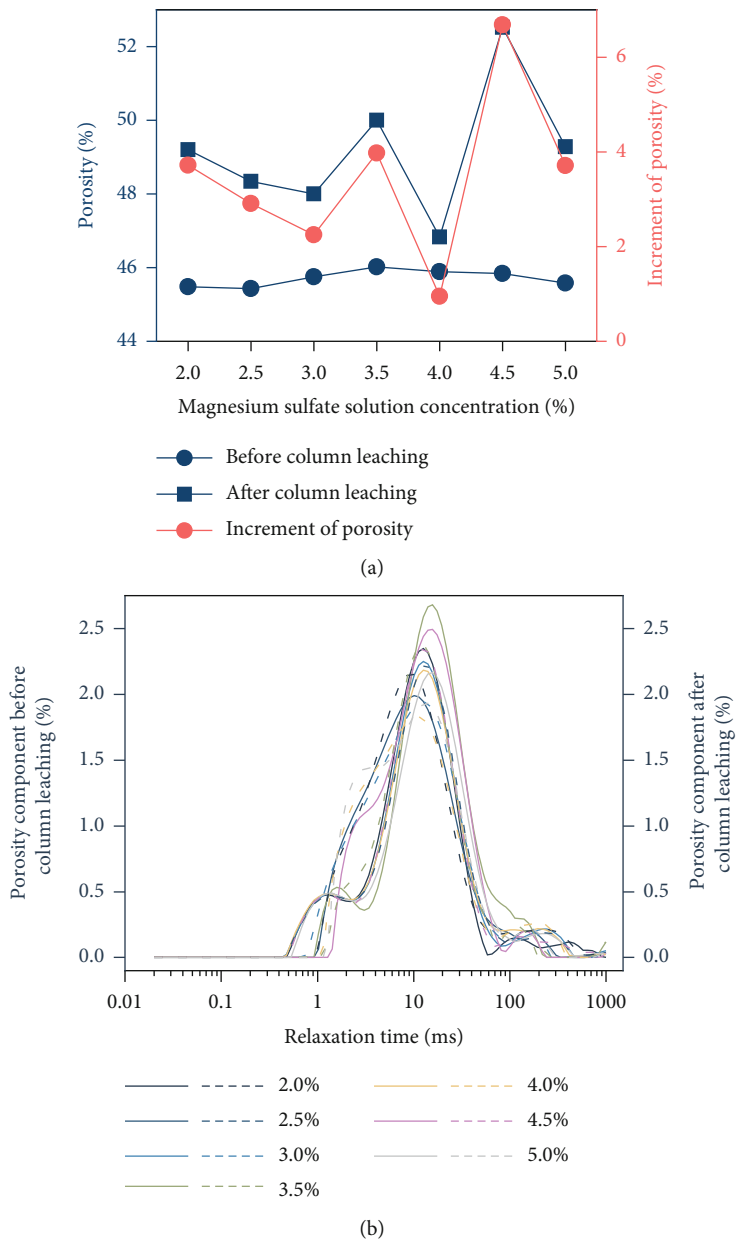

FIGURE 9: The concentration of leaching solution influences the porosity and the T_2 distribution curve of ore samples. (a) Percentage and increment of porosity before and after column leaching. (b) The T_2 distribution curve of porosity component before and after column leaching.

decreases, and the fractal dimension is elevated from 1.907 to 2.090, which indicates agglomerates are dispersed. When the solution's concentration turns from 3.5% to 5.0%, the viscous agglomerates decrease while micro agglomerates increase, and the fractal dimension is reduced from 2.090 to 1.927, which means the agglomerates are reunited. Figures 7(c), 7(d), and 8(b) show that when the pH of magnesium sulfate solution increased from 2 to 4, the percentage of viscous agglomerates decreased, accompanied by the increased micro agglomerates, and the fractal dimension dropped from 1.984 to 1.753 because of the reunited agglomerates. However, when the pH increased from 4 to 6, viscous agglomerates increased and micro agglomerates decreased, with the enhanced fractal dimension from 1.753 to 2.090; that is, the agglomerates are dispersed. For the ore sample with a particle size less than 0.075 mm, the critical magnesium sulfate solution concentration and pH that affect the stability of the agglomerates are 3.5% and 4, respectively.

3.3. The Pore Structure of Rare Earth Ore Influenced by the Concentration and pH of the Leaching Solution. Ion-absorbed rare earth deposits are affected by percolation and ion-exchange reactions during column leaching, which influence the stability of ore agglomerates and affect their internal microscopic pore structure and size. The pore

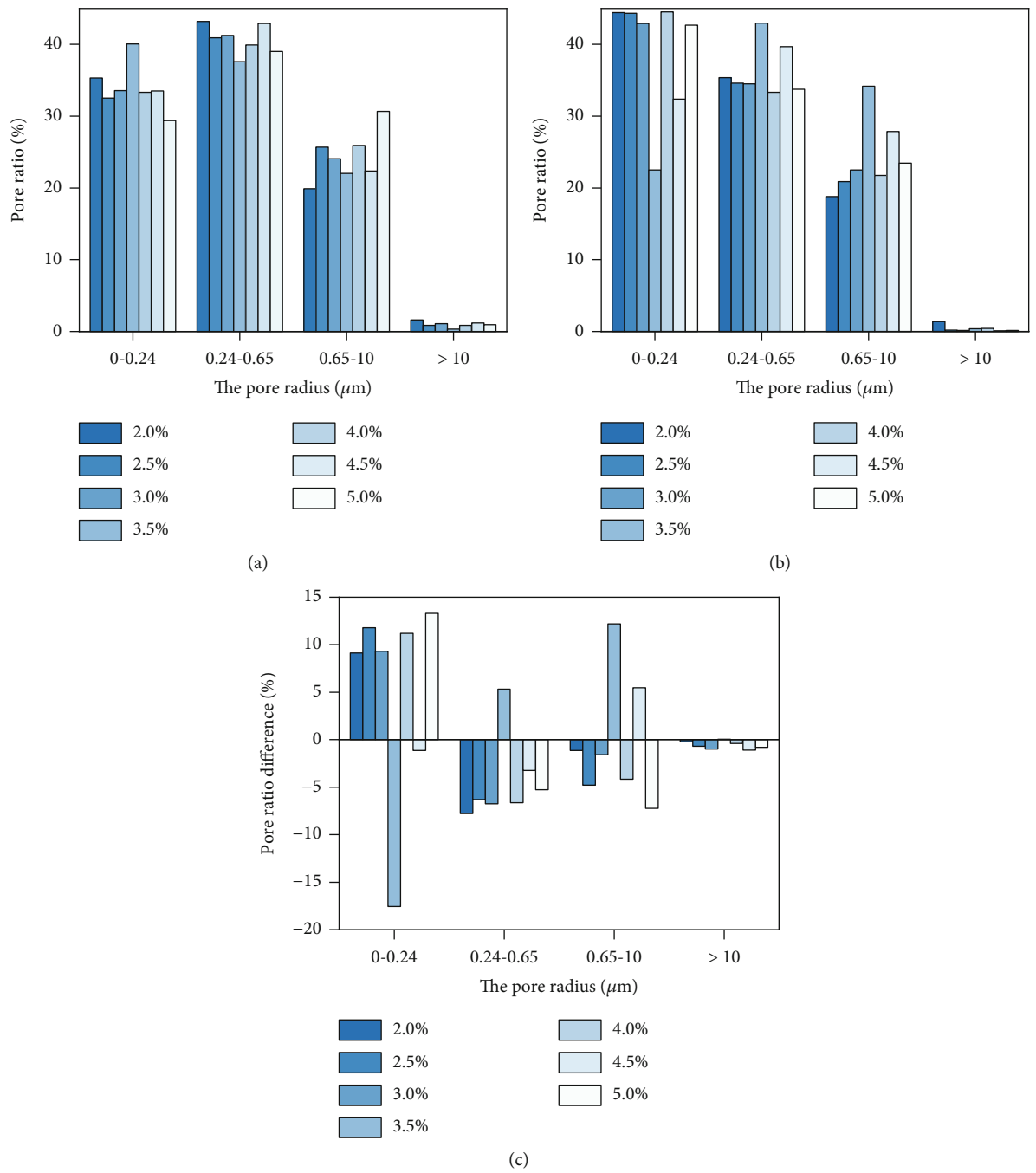

Figure 10: The concentration of leaching solution influences the proportion of ore samples' pores distribution. (a) The pore ratio before column leaching. (b) The pore ratio after column leaching. (c) Change of the pore ratio differences.

structure evolution inside the specimens before and after column leaching of different concentrations and pHs of magnesium sulfate solutions was investigated from a microscopic point of view by nuclear magnetic resonance imaging (NMR). According to the range of measured pore radius values, we divided pores into 4 categories: size range of 0-0.24 μm is called small pores, size range of 0.24-0.65 μm is called medium pores, size range of 0.65-10 μm is large pores, and radius greater than 10 μm is super pores. By analyzing the NMR T_2 distribution curve of the ore samples, the number of pores corresponding to the ore samples before and after column leaching shows significant differences. The pore size distribution of the ore samples before and after column leaching was also compared and analyzed, and the expression for the lateral relaxation time is shown as follows [36]:

$$\frac{1}{T_2} = \frac{1}{T_{2B}} + \rho_2\left(\frac{S}{V}\right) + \frac{D(\gamma \mathrm{GT}_E)^2}{12}. \quad (5)$$

In the equation, T_2 denotes the free relaxation time of the fluid in the tested sample, unit in ms; ρ_2 denotes the transverse

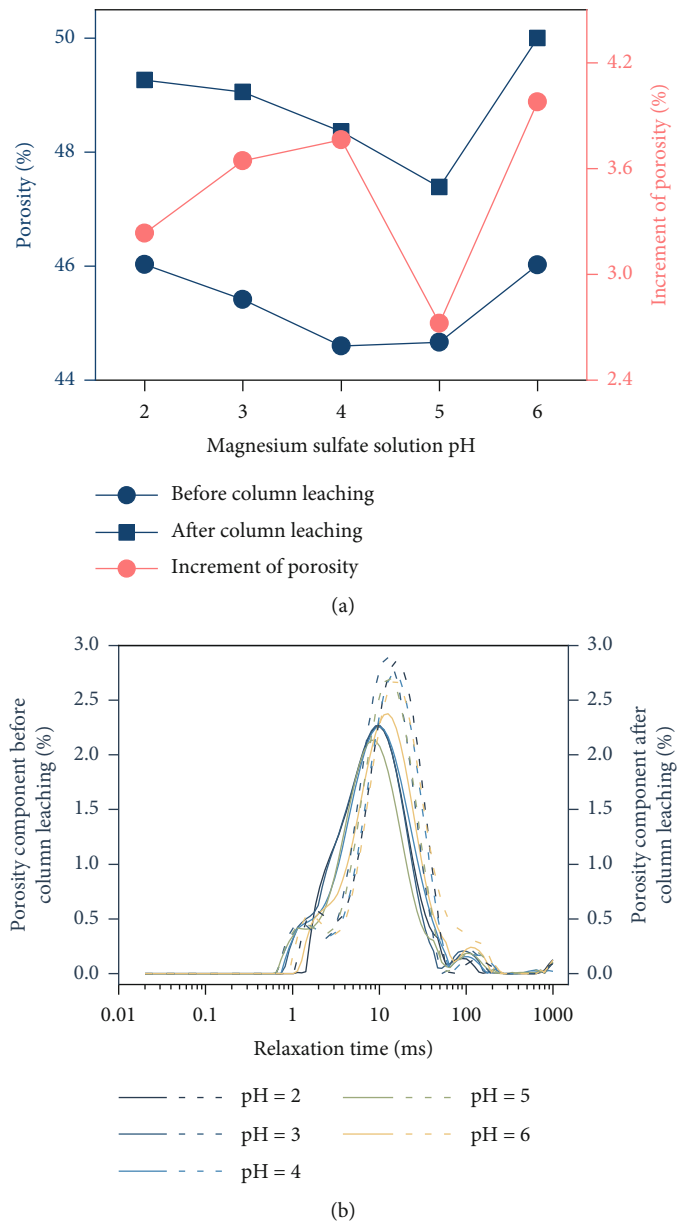

FIGURE 11: The pH of the leaching solution influence the porosity and the T_2 distribution curve of ore samples. (a) Percentage and increment of porosity before and after column leaching. (b) The T_2 distribution curve of porosity component before and after column leaching.

surface relaxation strength, unit in μm/ms; S is the surface area of the pore, unit in μm^2; V is the volume of the pore, unit in μm^3; D is the diffusion coefficient, (μm^2/ms); γ is the magnetic spin ratio, in $(T{\cdot}ms)^{-1}$; G is the magnetic field gradient, in 10^{-4}T/μm; and T_E is the echo interval, unit in ms.

The porosity change curve before and after column leaching is shown in Figure 9(a). The increase in porosity of the ore samples differed after column leaching than before under seven different concentrations of magnesium sulfate solution treatment. The largest increase in porosity is the concentration of 4.5% magnesium sulfate solution, the increase is up to 14.57%, and the porosity change is 6.680%; the next increase in porosity is the concentration of 3.5% with an increase of 8.64% and a porosity change of 3.978%; the smallest porosity increase is 2.07% under the 4.0% solution concentration treatment with a porosity change of 0.948%; the rest of the porosity change is basically similar. The reason for the different increase in porosity of the ore samples before and after column leaching is that the Mg^{2+} in the leaching solution reacts with the RE^{3+} on the surface of the clay ores by ion exchange, and a large amount of Mg^{2+} was adsorbed to the inner layer of the diffuse double layer due to the electrostatic effect, which changed the zeta potential of the particle surface and affected the diffuse double layer, that induced the stability change of the ore agglomerates. Meanwhile, the solution undergoes physical percolation in the ore sample, which makes the pore structure change and further increases its porosity.

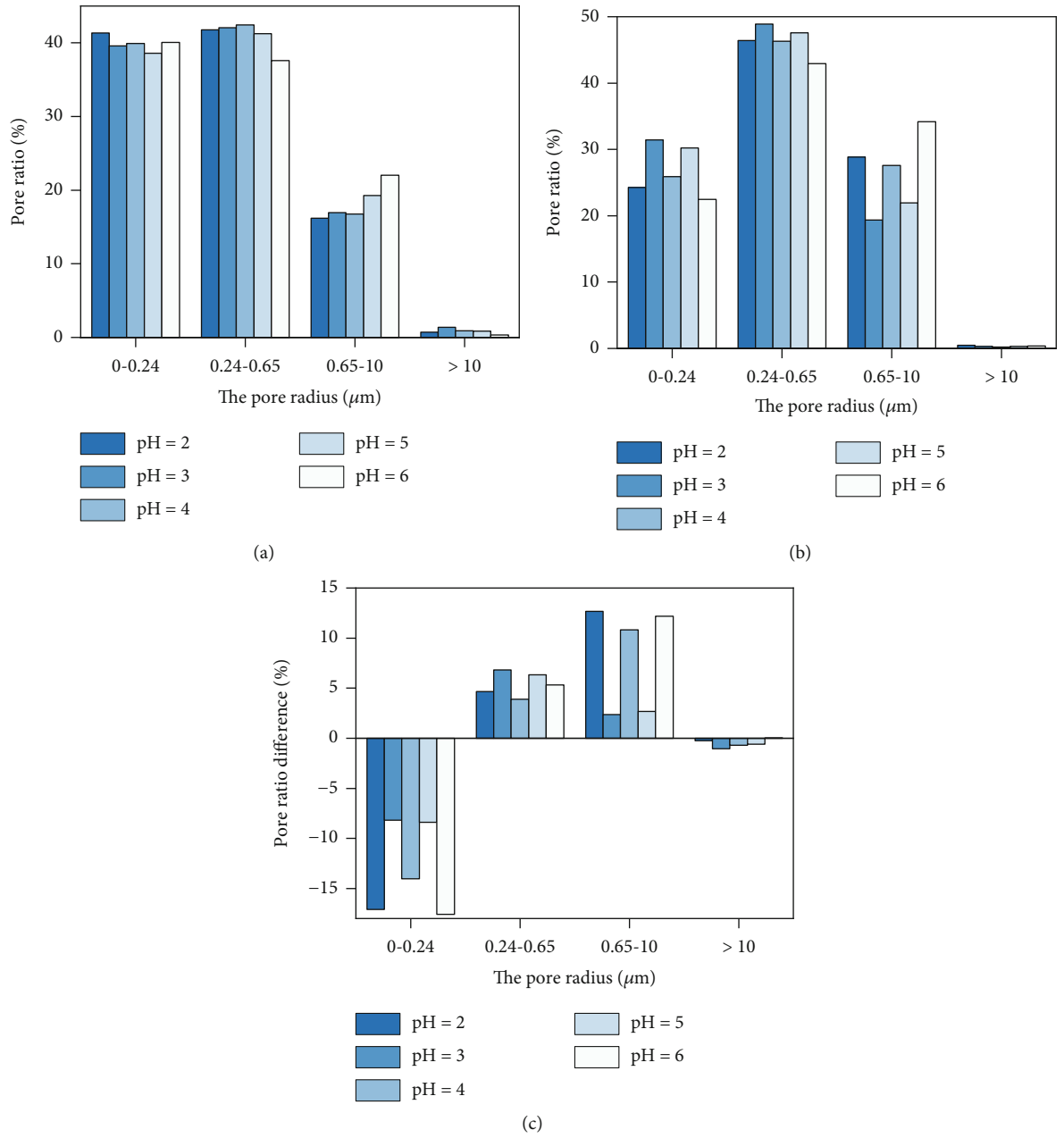

Figure 12: The pH of the leaching solution influence the proportion of ore samples' pores distribution. (a) The pore ratio before column leaching. (b) The pore ratio after column leaching. (c) Change of the pore ratio differences.

The NMR T_2 distribution curve of the ore samples before and after column leaching with different concentrations of magnesium sulfate solution is shown in Figure 9(b). The trends before and after column leaching are basically the same, which shows a slow rise at the beginning then a rapid rise to the peak, and finally, a decline to 0 with a small wave peak in the later stage. Compared to the T_2 curve before column leaching, the curve after leaching is continuously shifted to the left, which indicates that the pores are getting smaller after column leaching. Combined with the distribution of the pore radius ratio in Figure 10, it can be seen that the largest proportion is small and medium pores before and after column leaching, while the large pores increased along with the enhanced solutions' concentration. Figure 10(c) shows that the number of small pores is decreasing, while the number of medium pores and large pores is increasing after column leaching of magnesium sulfate solutions with concentrations of 3.5% and 4.5%, respectively. However, treatment with other concentrations of leaching solutions shows converse results, that is, increased small pores with decreased medium, large, and super pore numbers. When a strong ion exchange reaction happens, the small pores inside the ore sample rapidly increase, while the large pores and super pores decrease, indicating that the evolution of large pores and super pores toward small pores is mainly due to the compression and

reduction of the double electric layer thickness of clay particles under the strong ion exchange reaction when van der Waals gravity plays a dominant role and makes the clay particles closer to each other. And when the ion exchange reaction decelerates, the thickness of the double electric layer and the thickness of the sliding layer of the clay particles increases and the small pores evolve toward large and super pores as well. The change in the thickness of the sliding layer of the diffuse double electric layer in the soil particles leads to the instability of agglomerates and the alteration in the physical percolation of the leaching solution inside the ore sample, as well as the dispersion and agglomeration processes occurring in the coarse particles of the ore sample, which, combined with the modification of the particles, both affect the evolution of the internal pore of the ore sample.

Figure 11(a) shows the increase in porosity of the ore samples before and after column leaching under five different pHs of magnesium sulfate solution treatment. The largest increase in porosity occurs when the pH of magnesium sulfate solution is 6, which is up to 8.64% with a 3.978% variation of porosity; the smallest increase in porosity is 6.09% with 2.271% of the porosity variation after the leaching when the solution pH is 5. As the pH increased, the ore sample's porosity increment elevated, along with the porosity increase rate. The alteration of porosity in the ore sample before and after column leaching is mainly due to the saturation of deionized water in the early stage, which makes the originally unconnected pores in the soil sample connected to each other. The strong ion exchange reaction happens on the surface of clay ores when leaching with magnesium sulfate, which influences the surface zeta potential and results in a change in the sliding layer thickness of the diffuse double electric layer in soil particles. The agglomerate dispersion and agglomeration induce the physical percolation of the leaching solution inside the ore sample, which affects the pore evolution of the ore and increases its porosity. When increasing the acidity of magnesium sulfate, the -OH groups in some mineral components of the ore sample are dissolved, which induces the deposition of micro and viscous agglomerates and postpones the change in porosity. Meanwhile, the increased hydrogen ions in the leaching solution thicken the double electric layer of the clay ore, resulting in a change of pores inside the specimen.

The NMR T_2 distribution curve of the ore samples before and after column leaching with different pHs of magnesium sulfate solution is shown in Figure 11(b). The trends before and after column leaching are basically the same, which shows a slow rise in the beginning and then a rapid rise to the peak, and finally, a decline to 0 with a small wave peak in the later stage. Compared to the T_2 curve before column leaching, the curve after leaching is continuously shifted to the right, which indicates that the pores are getting bigger after column leaching. Combined with the distribution of the pore radius ratio in Figure 12, it can be seen that the largest proportion is small and medium pores before and after column leaching, while the large pores decreased along with the enhanced solutions' pH. Figure 12(c) shows that the number of small pores is decreasing, while the number of medium pores and large pores is increasing after column leaching. When a strong ion exchange reaction happens, the small pores inside the ore sample are rapidly decreasing, while the medium pores and large pores are increasing, indicating that the evolution of small pores is toward medium pores and large pores. This is mainly due to the broken equilibrium between the van der Waals gravity and the double electric layer repulsion under the strong ion exchange reaction, which leads to the increased double layer repulsion and thickness of the clay particles and further enhances the sliding layer thickness, resulting in the accelerated dispersion of agglomerates and more medium pores and large pores.

4. Conclusions

Based on the double electric layer and fractal theory, the thickness of the sliding layer and fractal dimension were calculated, as well as the stability of ion-absorbed rare earth deposit aggregates, which were analyzed during column leaching by magnesium sulfate solution of different concentrations and pHs. The main conclusions are as follows:

(1) With the increased concentration of magnesium sulfate solution, the absolute value of zeta potential on the surface of the particles undergoes a trend of increases toward decreases, in which the critical magnesium sulfate solution concentration that affects the stability of the ore sample agglomerates is 3.5%. When the concentration of magnesium sulfate solution increases from 2.0% to 3.5%, the thickness of the sliding layer on the surface of the ore sample particles increases, and the agglomerates are dispersed. When the solutions' concentration increases from 3.5% to 5.0%, the thickness of the sliding layer decreases, and the agglomerates are agglomerated

(2) With the increased pH of the magnesium sulfate solution, the zeta potential on the surface of the particles decreases and reaches its zero point potential at the pH of 3.5168. The critical magnesium sulfate solution at a pH of 4 affects the stability of ore agglomerates. When the magnesium sulfate solutions' pH increases from 2 to 4, the thickness of the sliding layer on the surface of the particles decreases, and the agglomerates are agglomerated. When the pH increases from 4 to 6, the thickness of the sliding layer increases, and the agglomerates are dispersed

(3) The incremental porosity of the ore samples after column leaching increased along with the increase in magnesium sulfate solutions' concentration and pH, as well as the porosity increase rate. Meanwhile, the balance of the van der Waals gravitational force and double layer repulsion between clay particles were broken, thus influencing the stability of agglomerates, which in turn caused the variability of different pore radius ratios of ore samples before and after column leaching

Data Availability

The data that support the findings of this study are available from the corresponding author (VS) upon reasonable request.

Conflicts of Interest

The authors declare that there is no conflict of interest regarding the publication of this paper.

Acknowledgments

This research was supported by the National Natural Science Foundation of China (51964014) and the Education Department of Jiangxi Province (GJJ209414).

References

[1] J. Tian, R. A. Chi, and J. Q. Yin, "Leaching process of rare earths from weathered crust elution-deposited rare earth ore," *Transactions of Nonferrous Metals Society of China*, vol. 20, no. 5, pp. 892–896, 2010.

[2] Q. Li, L. Qin, G. S. Wang, S. H. Luo, P. Long, and C. L. Peng, "Leaching mechanism of ion-adsorption rare earth," *Journal of the Chinese Society of Rare Earths*, vol. 39, no. 4, pp. 543–554, 2021.

[3] T. Qiu, H. Yan, J. Li, Q. Liu, and G. Ai, "Response surface method for optimization of leaching of a low-grade ionic rare earth ore," *Powder Technology*, vol. 330, 2018.

[4] G. A. Moldoveanu and V. G. Papangelakis, "Recovery of rare earth elements adsorbed on clay minerals: I. Desorption mechanism," *Hydrometallurgy*, vol. 117-118, pp. 71–78, 2012.

[5] D. Wang, Y. Rao, L. Shi, W. Xu, and T. Huang, "Relationship between permeability coefficient and fractal dimension of pore in ionic rare earth magnesium salt leaching ore," *Geofluids*, vol. 2022, Article ID 2794446, 13 pages, 2022.

[6] X. J. Yang, A. Lin, X.-L. Li, Y. Wu, W. Zhou, and Z. Chen, "China's ion-adsorption rare earth resources, mining consequences and preservation," *Environmental Development*, vol. 8, pp. 131–136, 2013.

[7] Q. Zhang, F. Ren, F. Li et al., "Ammonia nitrogen sources and pollution along soil profiles in an in-situ leaching rare earth ore," *Environmental Pollution*, vol. 267, p. 115449, 2020.

[8] Z. Y. He, Z. Y. Zhang, J. X. Yu, Z. Xu, and R.'a. Chi, "Process optimization of rare earth and aluminum leaching from weathered crust elution-deposited rare earth ore with compound ammonium salts," *Journal of Rare Earths*, vol. 34, no. 4, pp. 413–419, 2016.

[9] X. P. Luo, Y. B. Zhang, H. P. Zhou et al., "Pore structure characterization and seepage analysis of ionic rare earth orebodies based on computed tomography images," *International Journal of Mining Science and Technology*, vol. 32, no. 2, pp. 411–421, 2022.

[10] M. G. Sakellariou and M. D. Ferentinou, "A study of slope stability prediction using neural networks," *Geotechnical & Geological Engineering*, vol. 23, no. 4, pp. 419–445, 2005.

[11] S. Leguédois and Y. L. Bissonnais, "Size fractions resulting from an aggregate stability test, Interrill detachment and transport," *Earth Surface Processes and Landforms: The Journal of the British Geomorphological Research Group*, vol. 29, no. 9, pp. 1117–1129, 2004.

[12] C. Ao, P. L. Yang, W. Z. Zeng et al., "Impact of raindrop diameter and polyacrylamide application on runoff, soil and nitrogen loss via raindrop splashing," *Geoderma*, vol. 353, pp. 372–381, 2019.

[13] R. M. Ma, Z. X. Li, C. F. Cai, and J. G. Wang, "The dynamic response of splash erosion to aggregate mechanical breakdown through rainfall simulation events in Ultisols (subtropical China)," *Catena*, vol. 121, pp. 279–287, 2014.

[14] W. L. Zhang, B. Wang, Y. Q. Wang et al., "Quantitive transformation pathways of soil aggregate breakdown using rare earth element tracer method," *Journal of Soil and Water Conservation*, vol. 34, no. 2, pp. 154–169, 2020.

[15] X. F. Guo, G. H. Zhao, G. X. Zhang et al., "Effect of mixed chelators of EDTA, GLDA, and citric acid on bioavailability of residual heavy metals in soils and soil properties," *Chemosphere*, vol. 209, pp. 776–782, 2018.

[16] Z. H. Yu, J. B. Zhang, C. Z. Zhang, X. Xin, and H. Li, "The coupling effects of soil organic matter and particle interaction forces on soil aggregate stability," *Soil and Tillage Research*, vol. 174, pp. 251–260, 2017.

[17] D. Ma, H. Y. Duan, and J. X. Zhang, "Solid grain migration on hydraulic properties of fault rocks in underground mining tunnel: radial seepage experiments and verification of permeability prediction," *Tunnelling and Underground Space Technology incorporating Trenchless Technology Research*, vol. 126, article 104525, 2022.

[18] D. Ma, Q. Li, K. C. Cai et al., "Understanding water inrush hazard of weak geological structure in deep mine engineering: a seepage-induced erosion model considering tortuosity," *Journal of Central South University*, vol. 30, no. 2, pp. 517–529, 2023.

[19] D. Ma, S. B. Kong, Z. H. Li, Q. Zhang, Z. Wang, and Z. Zhou, "Effect of wetting-drying cycle on hydraulic and mechanical properties of cemented paste backfill of the recycled solid wastes," *Chemosphere*, vol. 282, article 131163, 2021.

[20] J. Caron, C. R. Espindola, and D. A. Angers, "Soil structural stability during rapid wetting: influence of land use on some aggregate properties," *Soil Science Society of America Journal*, vol. 60, no. 3, pp. 901–908, 1996.

[21] D. Curtin, H. Steppuhn, and F. Selles, "Effects of magnesium on cation selectivity and structural stability of sodic soils," *Soil Science Society of America Journal*, vol. 58, no. 3, pp. 730–737, 1994.

[22] K. Yilmaz, I. Çelik, S. Kapur, and J. Ryan, "Clay minerals, ca/mg ratio and Fe-Al-oxides in relation to structural stability, hydraulic conductivity and soil erosion in southeastern Turkey," *Turkish Journal of Agriculture & Forestry*, vol. 29, no. 1, pp. 29–37, 2005.

[23] Y. Liu, H. C. Liang, C. H. Tang, H. S. Cai, and J. W. Lju, "Inverse modeling of geochemical behavior of Ca^{2+} in landslide water-soil interaction system near the three gorges reservoir," *Hydrogeology and Engineering Geology*, vol. 39, no. 2, pp. 106–110, 2012.

[24] G. J. Levy and H. V. H. Van Der Watt, "Effect of exchangeable potassium on the hydraulic conductivity and infiltration rate of some south African soils," *Soil Science*, vol. 149, no. 2, pp. 69–77, 1990.

[25] Q. Z. Wang, X. Y. Liang, W. Wang et al., "Mineral composition and full-scale pore structure of Qianjiadian sandstone-type uranium deposits: application for in situ leaching mining," *Geofluids*, vol. 2022, Article ID 2860737, 15 pages, 2022.

[26] X. Y. Zhou, W. Wang, Q. H. Niu et al., "Geochemical reactions altering the mineralogical and multiscale pore characteristics of uranium-bearing reservoirs during CO^2 + O2in situ leaching," *Frontiers in Earth Science*, vol. 10, article 1094880, 2023.

[27] W. Wang, X. Y. Liang, Q. H. Niu et al., "Reformability evaluation of blasting-enhanced permeability in in situ leaching mining of low-permeability sandstone-type uranium deposits," *Nuclear Engineering and Technology*, vol. 55, no. 8, pp. 2773–2784, 2023.

[28] F. N. Hu, C. Y. Xu, H. Li et al., "Particles interaction forces and their effects on soil aggregates breakdown," *Soil and Tillage Research*, vol. 147, pp. 1–9, 2015.

[29] S. Li, H. Li, C. Y. Xu, X. R. Huang, D. T. Xie, and J. P. Ni, "Particle interaction forces induce soil particle transport during rainfall," *Soil Science Society of America Journal*, vol. 77, no. 5, pp. 1563–1571, 2013.

[30] H. Van, "An introduction to clay colloid chemistry," *Soil Science*, vol. 126, no. 1, p. 59, 1978.

[31] T. K. Sen and K. C. Khilar, "Review on subsurface colloids and colloid-associated contaminant transport in saturated porous media," *Advances in Colloid and Interface Science*, vol. 119, no. 2-3, pp. 71–96, 2006.

[32] J. Wang, G. S. Wang, and B. G. Hong, "Effects of concentration of pore solution on stability of ion-absorbed rare earth ore aggregate," *Advances in Civil Engineering*, vol. 2021, Article ID 8846605, 13 pages, 2021.

[33] W. Q. Ding, X. M. Liu, L. Song et al., "An approach to estimate the position of the shear plane for colloidal particles in an electrophoresis experiment," *Surface Science*, vol. 632, pp. 50–59, 2015.

[34] X. M. Liu, G. Yang, H. Li et al., "A theoretical exploration of the influencing factors for surface potential," *Chinese Physics B*, vol. 24, no. 6, article 068202, 2015.

[35] C. A. Cambardella and E. T. Elliott, "Carbon and nitrogen dynamics of soil organic matter fractions from cultivated grassland soils," *Soil Science Society of America Journal*, vol. 58, no. 1, pp. 123–130, 1994.

[36] N. R. A. Bird, A. R. Preston, E. W. Randall, W. R. Whalley, and A. P. Whitmore, "Measurement of the size distribution of water-filled pores at different matric potentials by stray field nuclear magnetic resonance," *European Journal of Soil Science*, vol. 56, no. 1, pp. 135–143, 2005.